

THEORETICAL STUDY ON THE MOLECULAR AND CRYSTAL STRUCTURES OF MYRICETIN

Hongchen Du¹, Rongkai Pan¹, Weiwei Huan^{2*}, Jie Li² and Lijuan Feng¹

¹Shandong Engineering Research Center of Green and High-Value Marine Fine Chemical, Weifang University of Science and Technology, Weifang 262700, China

²Zhejiang Provincial Key Laboratory of Chemical Utilization of Forestry Biomass, College of Chemistry and Materials Engineering, Zhejiang A&F University, Hangzhou 311300, China

(Received March 4, 2024; Revised May 30, 2024; Accepted June 4, 2024)

ABSTRACT. The molecular and crystal structures of myricetin have been studied using density functional theory. The geometry parameters are calculated based on the optimized molecular structure, and the thermodynamic properties “heat capacity ($C_{p,m}^{\ominus}$), enthalpy (H_m^{\ominus}) and entropy (H_m^{\ominus})” are performed using our self-programmed programme, the calculated results are consistent with literature reports. Crystal structures were predicted using the Dreiding force field and refined by DFT-GGA-RPBE method. The crystal form tends to crystalline in P-1 space group. The large calculated band gap (E_g) of the crystal proves it is stable, which is consistent with the conclusion from gas phase. The conduction band (LUCO) is mainly contributed from the p state of C atom and valence band (HOCO) from the p state of O atom.

KEY WORDS: Molecular structure, Crystal structure, Myricetin, Theoretical study

INTRODUCTION

Flavonoids are organic molecules from natural sources with interesting chemobiological and biophysical properties. Flavonoids are predominantly found in dietary sources and have therefore attracted much attention in applications such as functional foods, pharmaceutical preparations, catalysis and energy storage [1, 2]. Flavonoids are a class of polyphenolic secondary metabolites that are abundant in plants and foods. Flavonoids have a structural backbone of 15 carbon atoms consisting of two benzene rings (A and B) and a heterocycle (C). This carbon skeleton structure can be abbreviated as C6-C3-C6. Depending on the structure of the C-ring, they can be divided into different structural classifications such as flavonoids, flavonols, chalcones, isoflavonoids, anthocyanins, biflavonoids, and so on. The difference between the different structural classifications is the degree of oxidation and the substitution position of the C-ring. Flavonoids have a variety of biological activities, including antioxidant activity, free radical scavenging activity, prevention of coronary heart disease, hepatoprotective activity, anti-inflammatory and anticancer activity, while some flavonoids also have potential antiviral activity.

Myricetin is a hexahydroxyflavone corresponding to a flavonoid substituted with hydroxyl groups at positions 3, 3', 4', 5, 5' and 7 [3]. It has been shown to have anti-inflammatory, anti-allergic, anti-mutagenic and antioxidant activities [4-6]. Therefore, in recent years, many scientists have devoted themselves to studying the biological activity, especially the antioxidant activity of this compound, since free radical-induced membrane lipid peroxidation is believed to be associated with a wide range of chronic health problems such as cancer, atherosclerosis and ageing [7, 8].

There has been little systematic investigation of the molecular and crystal structures of myricetin because we know that most materials exist in condensed phases, especially in crystalline

*Corresponding authors. E-mail: vivid96@aliyun.com

This work is licensed under the Creative Commons Attribution 4.0 International License

form, and that many physical and chemical properties are closely related to crystal packing, and therefore crystal structure prediction of molecular geometries is of much greater value.

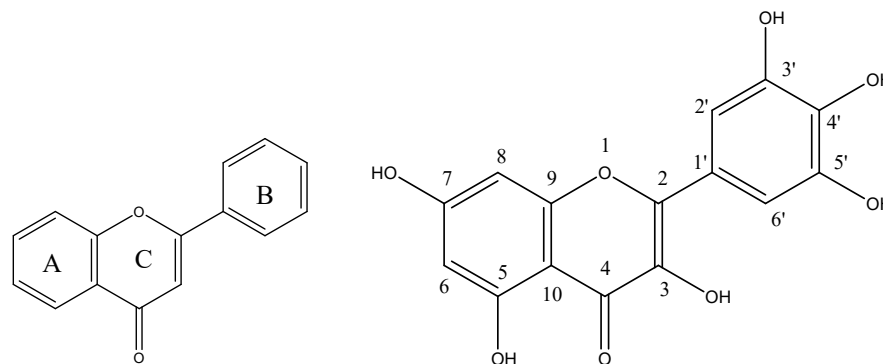


Figure 1. Flavonoid skeleton (left) and the molecular structure of myricetin with atomic number (right).

CALCULATION METHODS

Geometry optimizations and frequency calculations were carried out using the B3LYP functional in combination with the 6-311++g(d,p) basis set. The literature reports show that density functional methods are accurate and reliable in the study of organic compounds [9, 10].

According to the crystal statistics from the Cambridge Crystal Data Centre (CCDC), it is well known that a very small fraction of the 230 space groups are typical of organic crystals. It was found that most of the crystal lines belong to seven typical space groups, namely P21/c, P-1, P212121, Pbc_a, C2/c, P21, and Pna21 [11-15]. Prediction of the possible fillers was carried out as the following steps: (i) filling the crystal structure with asymmetric units and selecting low-energy fillers using a Monte Carlo simulated annealing procedure; (ii) performing a structure resulting from (i) clustering to eliminate duplicates; (iii) a geometrical optimisation step is carried out and the structure energy is minimised; (iv) the clusters of the iterative crystal structure are analysed and only the lowest energy representation of the cluster is retained, discarding the rest.

RESULTS AND DISCUSSIONS

Molecular structure

Figure 2 lists the optimized molecular structure of myricetin under B3LYP/6-311++g(d,p) level, the structural parameters such as bond lengths, bond angles and dihedral angles are given in Table 1.

We can see that the bond lengths of C-C in rings A and B are close to 1.4 Å, C8-C13 is the bond connecting ring B to chromone (rings A and C) of myricetin with a bond length of 1.473 Å, The conjugation between ring B and the chromone moiety and the conjugation in the heterocyclic ring C lead to a significant shortening of C8-C13 (about 1.473 Å), while the C1-C4 bond (1.464 Å) in ring C are larger than those in A and B, C4-C8 bond (1.362 Å) in ring C are close to the length of a normal benzene C-C bond (1.39 Å). The C1-O2 bond has a typical double bond character, while the other C-O bonds show typical single bond properties.

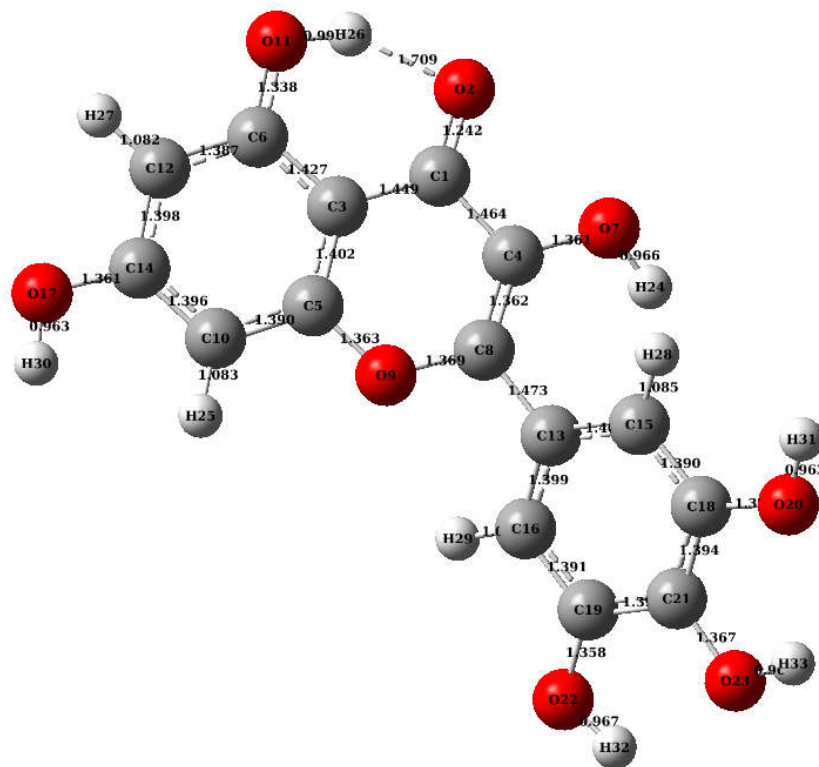


Figure 2. Structural parameters of myricetin obtained at the level of B3LYP/6-311++g(d,p) (bond lengths are in Å,).

Table 1. Optimized parameters for myricetin monomer (bond lengths in Å, bond and dihedral angles in degrees) obtained at the B3LYP/6-311++g(d,p) level.

Bond length		Bond angle		Dihedral angle	
C(1)-O(2)	1.242	O(2)-C(1)-C(3)	122.875	O(2)-C(1)-C(3)-C(5)	179.227
C(1)-C(3)	1.449	O(2)-C(1)-C(4)	122.107	O(2)-C(1)-C(3)-C(6)	0.283
C(1)-C(4)	1.464	C(3)-C(1)-C(4)	115.016	C(4)-C(1)-C(3)-C(5)	-0.16
C(3)-C(5)	1.402	C(1)-C(3)-C(5)	120.724	C(4)-C(1)-C(3)-C(6)	-179.103
C(3)-C(6)	1.427	C(1)-C(3)-C(6)	121.267	O(2)-C(1)-C(4)-O(7)	-2.187
C(4)-O(7)	1.361	C(5)-C(3)-C(6)	118.001	O(2)-C(1)-C(4)-C(8)	178.31
C(4)-C(8)	1.362	C(1)-C(4)-O(7)	115.132	C(3)-C(1)-C(4)-O(7)	177.205
C(5)-O(9)	1.363	C(1)-C(4)-C(8)	120.869	C(3)-C(1)-C(4)-C(8)	-2.298
C(5)-C(10)	1.39	O(7)-C(4)-C(8)	123.996	C(1)-C(3)-C(5)-O(9)	1.408
C(6)-O(11)	1.338	C(3)-C(5)-O(9)	120.617	C(1)-C(3)-C(5)-C(10)	-179.157
C(6)-C(12)	1.387	C(3)-C(5)-C(10)	122.517	C(6)-C(3)-C(5)-O(9)	-179.615
O(7)-H(24)	0.966	O(9)-C(5)-C(10)	116.864	C(6)-C(3)-C(5)-C(10)	-0.18
C(8)-O(9)	1.369	C(3)-C(6)-O(11)	120.311	C(1)-C(3)-C(6)-O(11)	-0.737
C(8)-C(13)	1.473	C(3)-C(6)-C(12)	120.183	C(1)-C(3)-C(6)-C(12)	179.185
C(10)-C(14)	1.396	O(11)-C(6)-C(12)	119.505	C(5)-C(3)-C(6)-O(11)	-179.709
C(10)-H(25)	1.083	C(4)-O(7)-H(24)	109.468	C(5)-C(3)-C(6)-C(12)	0.214

C(12)-C(14)	1.398	C(4)-C(8)-O(9)	121.804	C(1)-C(4)-O(7)-H(24)	-165.876
C(12),H(28)	7.349	C(4)-C(8)-C(13)	125.752	C(8)-C(4)-O(7)-H(24)	13.609
C(13)-C(15)	1.407	O(9)-C(8)-C(13)	112.401	C(1)-C(4)-C(8)-O(9)	3.624
C(13)-C(16)	1.399	C(5)-O(9)-C(8)	120.883	C(1)-C(4)-C(8)-C(13)	-178.953
C(14)-O(17)	1.361	C(5)-C(10)-C(14)	117.799	O(7)-C(4)-C(8)-O(9)	-175.833
C(15)-C(18)	1.39	C(5)-C(10)-H(25)	119.98	O(7)-C(4)-C(8)-C(13)	1.59
C(15),H(29)	3.415	C(14)-C(10)-H(25)	122.22	C(3)-C(5)-O(9)-C(8)	-0.226
C(16)-C(19)	1.391	C(6)-C(12)-C(14)	119.584	C(10)-C(5)-O(9)-C(8)	-179.692
C(16),H(30)	6.971	C(6)-C(12),H(28)	42.666	C(3)-C(5)-C(10)-C(14)	0.053
O(17),H(31)	10.606	C(14)-C(12),H(28)	78.521	C(3)-C(5)-C(10)-H(25)	-179.62
C(18)-O(20)	1.373	C(8)-C(13)-C(15)	120.33	O(9)-C(5)-C(10)-C(14)	179.508
C(18)-C(21)	1.394	C(8)-C(13)-C(16)	119.823	O(9)-C(5)-C(10)-H(25)	-0.165
C(19)-C(21)	1.398	C(15)-C(13)-C(16)	119.843	C(3)-C(6)-C(12)-C(14)	-0.125
C(19)-O(22)	1.358	C(10)-C(14)-C(12)	121.915	C(3)-C(6)-C(12),H(28)	17.395
O(20),H(32)	4.612	C(10)-C(14)-O(17)	121.652	O(11)-C(6)-C(12)-C(14)	179.799
C(21)-O(23)	1.367	C(12)-C(14)-O(17)	116.432	O(11)-C(6)-C(12),H(28)	-162.681
O(22),H(33)	3.672	C(13)-C(15)-C(18)	119.504	C(4)-C(8)-O(9)-C(5)	-2.337
O(23),H(27)	11.496	C(13)-C(15),H(29)	21.195	C(13)-C(8)-O(9)-C(5)	179.925
		C(18)-C(15),H(29)	98.312	C(4)-C(8)-C(13)-C(15)	43.286
		C(13)-C(16)-C(19)	120.12	C(4)-C(8)-C(13)-C(16)	-137.52
		C(13)-C(16),H(30)	84.96	O(9)-C(8)-C(13)-C(15)	-139.083
		C(19)-C(16),H(30)	143.986	O(9)-C(8)-C(13)-C(16)	40.112
		C(14)-O(17),H(31)	30.341	C(5)-C(10)-C(14)-C(12)	0.044
		C(15)-C(18)-O(20)	124.625	C(5)-C(10)-C(14)-O(17)	-179.908
		C(15)-C(18)-C(21)	120.632	H(25)-C(10)-C(14)-C(12)	179.709
		O(20)-C(18)-C(21)	114.739	H(25)-C(10)-C(14)-O(17)	-0.242
		C(16)-C(19)-C(21)	120.079	C(6)-C(12)-C(14)-C(10)	-0.007
		C(16)-C(19)-O(22)	119.685	C(6)-C(12)-C(14)-O(17)	179.947
		C(21)-C(19)-O(22)	120.235	H(28),C(12)-C(14)-C(10)	-12.023
		C(18)-O(20),H(32)	45.524	H(28),C(12)-C(14)-O(17)	167.931
		C(18)-C(21)-C(19)	119.814	C(8)-C(13)-C(15)-C(18)	179.837
		C(18)-C(21)-O(23)	122.61	C(8)-C(13)-C(15),H(29)	178.787
		C(19)-C(21)-O(23)	117.573	C(16)-C(13)-C(15)-C(18)	0.642
		C(19)-O(22),H(33)	58.172	C(16)-C(13)-C(15),H(29)	-0.407
		C(21)-O(23),H(27)	12.783	C(8)-C(13)-C(16)-C(19)	-179.906
				C(8)-C(13)-C(16),H(30)	-27.333
				C(15)-C(13)-C(16)-C(19)	-0.707
				C(15)-C(13)-C(16),H(30)	151.866
				C(10)-C(14)-O(17),H(31)	23.24
				C(12)-C(14)-O(17),H(31)	-156.714
				C(13)-C(15)-C(18)-O(20)	-179.209
				C(13)-C(15)-C(18)-C(21)	0.056
				H(29),C(15)-C(18)-O(20)	-178.825
				H(29),C(15)-C(18)-C(21)	0.439
				C(13)-C(16)-C(19)-C(21)	0.073
				C(13)-C(16)-C(19)-O(22)	-179.628
				H(30),C(16)-C(19)-C(21)	-128.635
				H(30),C(16)-C(19)-O(22)	51.664
				C(15)-C(18)-O(20),H(32)	178.92
				C(21)-C(18)-O(20),H(32)	-0.383
				C(15)-C(18)-C(21)-C(19)	-0.69
				C(15)-C(18)-C(21)-O(23)	179.886
				O(20)-C(18)-C(21)-C(19)	178.644
				O(20)-C(18)-C(21)-O(23)	-0.78

				C(16)-C(19)-C(21)-C(18)	0.624
				C(16)-C(19)-C(21)-O(23)	-179.923
				O(22)-C(19)-C(21)-C(18)	-179.676
				O(22)-C(19)-C(21)-O(23)	-0.224
				C(16)-C(19)-O(22),H(33)	-179.95
				C(21)-C(19)-O(22),H(33)	0.349
				C(18)-C(21)-O(23),H(27)	145.304
				C(19)-C(21)-O(23),H(27)	-34.132

The HOMO (highest occupied molecular orbital) represents the ability to donate an electron as an electron donor, electron as an electron acceptor; the LUMO (lowest unoccupied molecular orbital) represents the ability to the ability to accept an electron. The smaller the HOMO and LUMO gaps, the electrons are easily excited from the HOMO and it is easy for the LUMO to accept these electrons. Based on the calculated results, the HOMO-LUMO gap of myricetin is 4.02 eV, which indicates that it is stable at room temperature and pressure.

We calculated the HOMO and LUMO using Multiwfn programme [16], Figure 3 shows the HOMO of myricetin, and it shows the characteristic of the π state. For myricetin, the HOMO remains mostly on the A and C rings and in the C4-C8 double bond, indicating that the hydroxides in the A and C rings have strong antioxidant activity, while the LUMO remains mostly on the C1-C4 and C8-C13 bonds, which is in good agreement with previous calculated results.

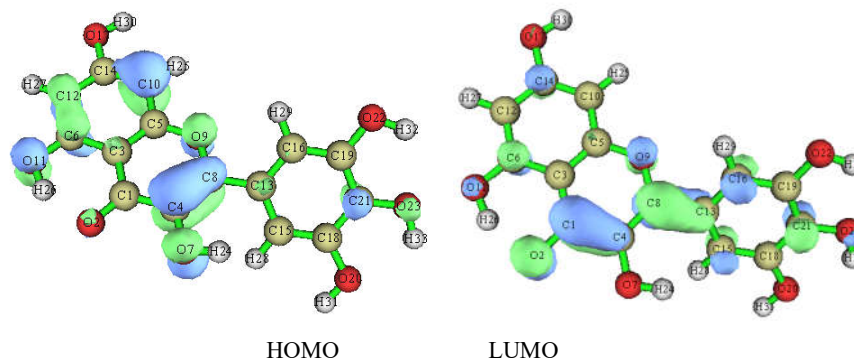


Figure 3. Frontier molecular orbitals of myricetin.

Thermodynamic properties

Based on the scaled vibrational frequencies and the principle of statistical thermodynamics, the standard thermodynamic properties are evaluated and shown in Figure 4. Obviously, as the temperature increases, all the thermodynamic properties increase, mainly because the vibrational motion is intensified at the higher temperature and therefore contributes more to the thermodynamic properties. The relationships between the thermodynamic functions and temperature are found and shown as follows (the units of $C_{p,m}^{\ominus}$, S_m^{\ominus} , and H_m^{\ominus} are $\text{J}\cdot\text{K}^{-1}\cdot\text{mol}^{-1}$, $\text{J}\cdot\text{K}^{-1}\cdot\text{mol}^{-1}$, $\text{kJ}\cdot\text{mol}^{-1}$, respectively, and the correlation coefficients are 0.9996, 1, and 0.9998 respectively):

$$C_{p,m}^{\ominus} = 19.68 + 1.28 T - (6.84 \times 10^{-4}) T^2$$

$$S_m^{\ominus} = 233.83 + 1.38 T - (3.98 \times 10^{-4}) T^2$$

$$H_m^{\ominus} = -22.87 + 0.17 T + (2.94 \times 10^{-4}) T^2$$

From these equations, we have

$$\frac{dC_{p,m}^{\circ}}{dT} = 1.28 - (13.68 \times 10^{-4})T$$

$$\frac{dS_m^{\circ}}{dT} = 1.38 - (7.96 \times 10^{-4})T$$

$$\frac{dH_m^{\circ}}{dT} = 0.17 + (5.88 \times 10^{-4})T$$

Obviously, with the increase of temperature, the increase of $C_{p,m}^{\circ}$ and S_m° decrease, while that of H_m° increases. Under the room temperature (298.15 K), the calculated $C_{p,m}^{\circ}$, S_m° , and H_m° of myricetin is $340.51 \text{ J}\cdot\text{K}^{-1}\cdot\text{mol}^{-1}$, $621.76 \text{ J}\cdot\text{K}^{-1}\cdot\text{mol}^{-1}$, and $53.95 \text{ kJ}\cdot\text{mol}^{-1}$, respectively.

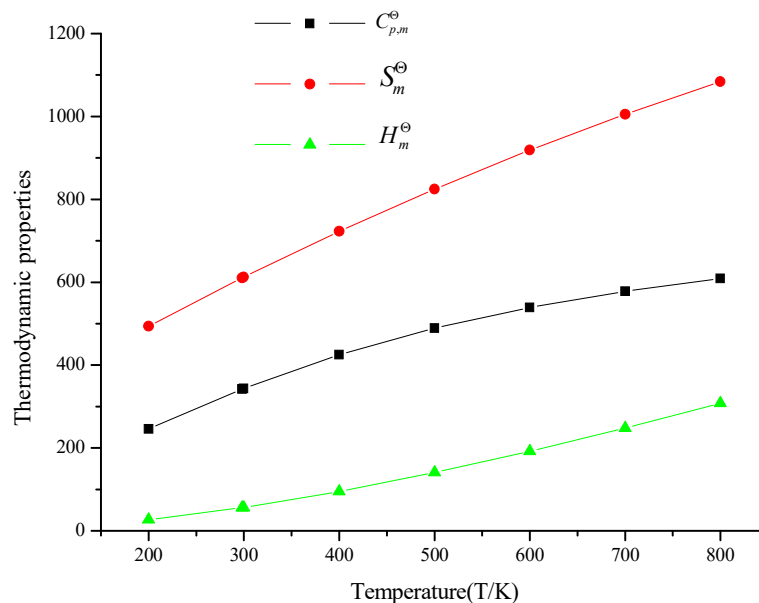


Figure 4. The thermodynamic properties of myricetin.

Crystal structures

The predicted energies (E), cell parameters (a , b , c , α , β , γ), and densities (ρ) of the most possible crystal structures using Dreiding force field method are listed in Table 2. We can see that different packing forms have different energies and densities, the energies of various packings obtained with Dreiding force field are in $5.93\sim 10.46 \text{ kcal}\cdot\text{mol}^{-1}\cdot\text{cell}^{-1}$. According to the principle that the possible stable polymorph usually possesses a lower energy, the crystal structure of myricetin belongs more probably to the $P-1$ group.

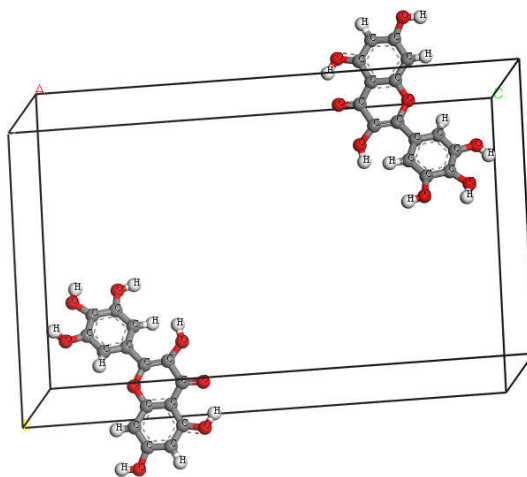
Table 2. Possible molecular packings for myricetin in seven most possible space groups from the Dreiding force field.

Space groups	<i>C2/C</i>	<i>P-1</i>	<i>P2₁</i>	<i>P2₁/c</i>	<i>P2₁2₁2₁</i>	<i>Pbca</i>	<i>Pna2₁</i>
<i>Z</i>	8	2	2	4	4	8	4
$\rho(\text{g}\cdot\text{cm}^{-3})$	1.63	1.64	1.62	1.63	1.63	1.59	1.66
$E(\text{kcal}\cdot\text{mol}^{-1}\cdot\text{cell}^{-1})$	7.37	5.93	8.10	6.37	8.45	10.46	8.26
<i>a</i> (Å)	64.37	7.63	3.68	3.75	7.12	11.66	13.32
<i>b</i> (Å)	3.66	3.76	13.41	50.20	49.51	7.90	13.04
<i>c</i> (Å)	14.25	29.14	13.21	8.12	3.67	28.96	7.34
$\alpha(^{\circ})$	90.00	76.72	90.00	90.00	90.00	90.00	90.00
$\beta(^{\circ})$	50.62	58.66	85.06	58.29	90.00	90.00	90.00
$\gamma(^{\circ})$	90.00	64.62	90.00	90.00	90.00	90.00	90.00

The selected crystal structures were further optimized using DFT-GGA method (Figure 5), the equilibrium structure of the title compounds were obtained by full relaxation of the unit cell parameters allowed by *P-1* crystal symmetry as well as of the atomic positions inside the unit cell, Table 3 lists the optimized lattice parameters, the obtained lattice parameters are $a=4.86$ Å, $b=17.09$ Å, $c=29.53$ Å, $\alpha=92.00^{\circ}$, $\beta=53.10^{\circ}$, $\gamma=118.80^{\circ}$, $Z=2$, $\rho=2.46$ g·cm⁻³.

Table 3. The optimized crystal structure parameters using DFT-GGA-RPBE method.

Space groups	myricetin
<i>Z</i>	4
<i>a</i> (Å)	4.86
<i>b</i> (Å)	17.09
<i>c</i> (Å)	29.53
$\alpha(^{\circ})$	92.00
$\beta(^{\circ})$	53.10
$\gamma(^{\circ})$	118.80
$\rho(\text{g}\cdot\text{cm}^{-3})$	2.36

Figure 5. The optimized crystal structures of myricetin in *P-1* space group.

Band gap

The band gap is an important parameter used to characterize the electronic structure of crystals and generally refers to the energy difference (in electron volts) between the top of the valence band (HOCO) and the bottom of the conduction band (LUCO) in insulators and semiconductors. This is equivalent to the energy required to free an outer shell electron from its orbit around the nucleus to become a mobile charge carrier, able to move freely within the solid material. Compounds with large band gaps are generally insulators, those with smaller band gaps are semiconductors, while conductors have either very small band gaps or none because the valence and conduction bands overlap. It is related to impact sensitivity and can be used as a criterion to predict the sensitivity of energetic materials with similar structure. Based on the equilibrium crystal structures of the title compounds obtained at the GGA-RPBE level, the self-consistent band structure along different symmetry directions of the Brillouin zone was calculated and analysed.

From Figure 6, it can be seen that in myricetin, the variation of the limit band with the k-value becomes steeper in the direction of the reciprocal vector of the Brillouin range. The band gap is 2.5 eV, which means that it is a semiconductor.

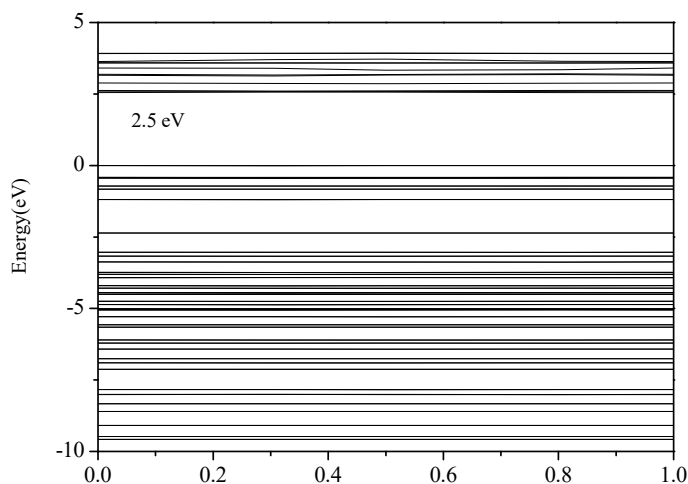


Figure 6. The energy bands at ambient pressure along the different symmetric direction of the Brillouin zone. The Fermi energy is shown as a dashed horizontal line.

Density of states (DOS)

In order to obtain more information about the bonding nature of the title compounds, the total electronic density of states and the partial DOS (PDOS) are calculated and shown in Figure 5. The density of states (DOS) is a representation of the band structure of a crystal and can reveal the composition of the valence band (HOCO) and the conduction band (LUCO). A better understanding of the band structure is provided by the partial density of states (PDOS), where the DOS is projected onto the atom-centred orbital and can be used to investigate the constitution of the energy bands. From Figure 5 it can be seen that the DOS are finite at the Fermi energy level

because the DOS contain some form of broadening effect. In the upper valence bands, the title compounds have a sharp peak near the Fermi level, indicating that the upper valence band of the band structures are flat, all peaks are predominantly from the p states. Also, several main peaks of the upper valence band are superimposed by the s and p states. The conduction bands are also dominated by the p states, indicating that the p states play an important role in their chemical reaction.

Analysing the DOS and PDOS of the crystal structures with P-1 symmetry shown in Figure 7, it can be seen that in myricetin, LUCO is mainly contributed by the p-state of the C atom, while HOCO is mainly composed of the p-states of the O atom.

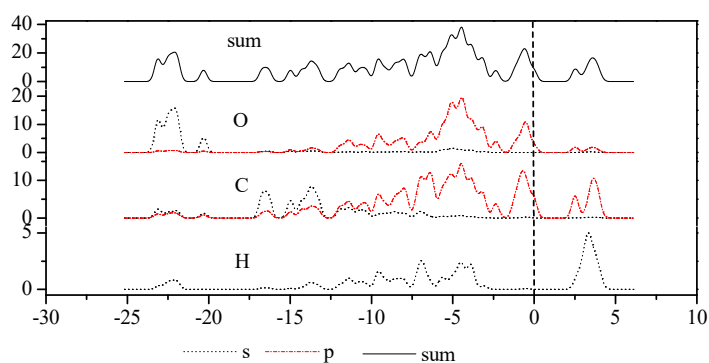


Figure 7. The energy bands at ambient pressure along the different symmetric direction of the Brillouin zone. The Fermi energy is shown as a dashed horizontal line.

ACKNOWLEDGMENTS

We wish to thank Nanjing University of Science and Technology for the computational assistance.

FUNDINGS

This work was supported by National Natural Science Foundation of China (52301100, 32371809,); Key R&D Projects of Zhejiang Province in 2021 (2021C02013); Zhejiang Province "Three Rural Nine Parties" Science and Technology Collaboration Programme (2022SNJF059); Weifang Science and Technology Development Plan (2022GX035, 2022GX033, 2023GX058); and Weifang University of Science and Technology High-level Talent Startup Project (KJRC2022006, KJRC2022005, KJRC2019014).

AUTHORS CONTRIBUTION

The first two authors contributed equally to this work.

REFERENCES

1. Yousefi, M.; Shadnoush, M.; Sohrabvandi, S.; Khorshidian, N.; Mortazavian, A.M. Encapsulation systems for delivery of flavonoids: A review. *Biointerface Res. App. Chem.* **2021**, *11*, 13934-13951.
2. de Oliveira Salles, R.C.; Muniz, M.P.; Nunomura, R.D.C.S.; Nunomura, S.M. Geographical origin of guarana seeds from untargeted UHPLC-MS and chemometrics analysis. *Food Chem.* **2022**, *371*, 131068.
3. Semwal, D.K.; Semwal, R.B.; Combrinck, S.; Viljoen, A. Myricetin: A dietary molecule with diverse biological activities. *Nutrients* **2016**, *8*, 90.
4. Ko, C.H.; Shen, S.C.; Lee, T.J.; Chen, Y.C. Myricetin inhibits matrix metalloproteinase 2 protein expression and enzyme activity in colorectal carcinoma cells. *Mol. Cancer Ther.* **2005**, *4*, 281-290.
5. Morales, P.; Haza, A.I. Selective apoptotic effects of piceatannol and myricetin in human cancer cells. *J. Appl. Toxicol.* **2012**, *32*, 986-993.
6. Rasulev, B.F.; Abdullaev, N.D.; Syrov, V.N.; Leszczynski, J. A quantitative structure-activity relationship (QSAR) study of the antioxidant activity of flavonoids. *QSAR Comb. Sci.* **2005**, *24*, 1056-1065.
7. DeToma, A.S.; Choi, J.S.; Braymer, J.J.; Lim, M.H. Myricetin: A naturally occurring regulator of metal-induced amyloid- β aggregation and neurotoxicity. *ChemBioChem* **2011**, *12*, 1198-1201.
8. Delgado, M.E.; Haza, A.I.; García, A.; Morales, P. Myricetin, quercetin, (+)-catechin and (-)-epicatechin protect against N-nitrosamines-induced DNA damage in human hepatoma cells. *Toxicol. In Vitro*, **2009**, *23*, 1292-1297.
9. Huan, W.; Du, H.; Pan, R.; Li, J.; Feng, L. Theoretical study on glucose and methylamine Maillard reaction: formation of the Amadori rearrangement products. *Bull. Chem. Soc. Ethiop.* **2024**, *38*, 539-545.
10. Rafik, A.; Zouihri, H.; Guedira, T. Hirshfeld surface analysis and quantum chemical study of molecular structure of phosphate. *Bull. Chem. Soc. Ethiop.* **2021**, *35*, 625-638.
11. Chernikova, N.Y.; Bel'skii, V.K.; Zorkii, P.M. New statistical data on the topology of homomolecular organic crystals. *J. Struct. Chem.* **1990**, *31*, 661-666.
12. Mighell, A.D.; Himes, V.L.; Rodgers, J.R. Space-group frequencies for organic compounds. *Acta Crystallogr. A* **1983**, *39*, 737-740.
13. Wilson, A.J.C. Space groups rare for organic structures. I. Triclinic, monoclinic and orthorhombic crystal classes. *Acta Crystallogr. A* **1988**, *44*, 715-724.
14. Srinivasan, R. On space-group frequencies. *Acta Crystallogr. A* **1992**, *48*, 917-918.
15. Baur, W.H.; Kassner, D. The perils of Cc: comparing the frequencies of falsely assigned space groups with their general population. *Acta Crystallogr. B* **1992**, *48*, 356-369.
16. Lu, T.; Chen F.; Multiwfn: A multifunctional wavefunction analyzer, *J. Comput. Chem.* **2012**, *33*, 580-592.